

Order parameter and spectral function in d -wave holographic superconductors

Debabrata Ghorai^{✉,*}, Taewon Yuk^{✉,†} and Sang-Jin Sin^{✉,‡}
Department of Physics, Hanyang University, Seoul 04763, Korea

 (Received 7 January 2024; accepted 15 February 2024; published 5 March 2024)

We consider the d -wave holographic superconductor model with full backreaction on the metric, addressing a missing part in the literature. We have identified the gap function by comparing the fermionic spectral function with the momentum-dependent order parameter. By numerical investigations of the fermionic spectral function in the presence of a tensor condensate, we find the Fermi arc and the gapped behavior, which closely resembles angle resolved photoemission spectrum data. Moreover, we have examined the influence of the coupling constant, chemical potential, and temperature on the spectral function. We find that d -wave fermionic spectral function can be obtained through p_x and p_y condensates combined with two fermion flavors. Similarly, combining $d_{x^2-y^2}$ and d_{xy} orbitals symmetry with two fermion flavors leads to a g -wave spectral function.

DOI: [10.1103/PhysRevD.109.066004](https://doi.org/10.1103/PhysRevD.109.066004)

I. INTRODUCTION

Angle resolved photoemission spectrum (ARPES) data [1] indicates that most unconventional superconductors exhibit d -wave orbital symmetry. However, understanding the theoretical aspects of these systems remains elusive due to the limitations of conventional methods in describing strongly coupled systems. To address this, the gauge/gravity duality [2–4] offers an approach by employing a weakly coupled dual system in one higher dimension [5–13]. The relationship between the energy gap and the critical temperature of high T_c superconductors [14] has been given in [15] in the simplest dual gravitational system [16] with scalar hair. This system exhibits a second-order phase transition from anti-de Sitter (AdS)-Schwarzschild geometry to hairy black hole geometry and is referred to as s -wave holographic superconductors, characterized by an isotropic energy gap. To include anisotropic gap function in holographic superconductors, we need p -wave and d -wave gaps that had been realized in spin-one fields [17–19]) and tensor fields [20–26], respectively.

Considerable amount of works [27–48] have been done using gravitons and photons in the bulk. Although less attention has been paid to the fermionic side, there have been some works on the fermion spectral function, exhibiting

distinct spectral features in the presence of the scalar [49,50], vector [18,51], and tensor [20,21,52,53] condensations. The presence of some of such condensations gives rise to the Fermi arc for p - and d -wave holographic superconductors. In the case of spin-two fields, the Lagrangian density becomes somewhat intricate. The initial formulation of d -wave holographic superconductivity [21] did not treat the number of degrees of freedom properly. Based on earlier investigations on the spin two fields [54,55], the formulation of an proper action for a massive charged spin two field was accomplished by Benini, Herzog, Rahman, and Yarom in [20], by employing the Einstein condition that forbids the backreaction, so that in their setup we have to investigate d -wave holographic superconductors in the probe limit only. However, the full backreacted geometry [41,56,57] can play an important role [58].

In this paper, we reformulate the Benini, Herzog, Rahman, and Yarom Lagrangian by replacing the Einstein condition with the traceless condition in the constraint equation for spin-two fields. This allows the presence of the backreaction of tensor condensate to the metric. Another concern in d -wave holographic superconductors is about the momentum dependence of the order parameter, which should be consistent with that of the fermion spectral function. In all previous computations, the order parameter was considered as B_{xx} , which is independent of the momentum direction. One of our aims here is to identify the precise d -wave order parameter that has angular dependence in momentum space consistent with that of the fermion spectral function. We will identify the correct d -wave order parameter as $B_{\rho\rho}$ where ρ is the radial direction in the xy plane. The detailed analysis of the Fermi arc in the presence of the d -wave gap and full backreaction is presented here for various orbital symmetries. We also examine the effect of coupling strength, the chemical potential and temperature on

*dghorai123@gmail.com

†tae1yuk@gmail.com

‡sangjin.sin@gmail.com

Published by the American Physical Society under the terms of the [Creative Commons Attribution 4.0 International license](https://creativecommons.org/licenses/by/4.0/). Further distribution of this work must maintain attribution to the author(s) and the published article's title, journal citation, and DOI. Funded by SCOAP³.

the spectral function. We have shown that the d -wave spectral function can be obtained from the two different p -wave condensates with two fermion flavors. Similarly, two fermion flavors with condensates of two different tensor fields lead to g -wave spectral function. These may be useful to describe higher orbital superconductivity.

This paper is organized as follows. In Sec. II, we argue that one can construct a Lagrangian density without imposing the Einstein condition. This allows the presence of the backreaction of matter fields on the background geometry. In Sec. III, we numerically investigate the critical temperature and all bosonic configurations. In Sec. IV, we describe how to calculate the boundary fermion Green's function using the flow equation. In Sec. V, we analyze the spectral function of various cases. We summarize and conclude in Sec. VI.

II. BASIC SETUP FOR SPIN-TWO FIELD

The Fierz-Pauli Lagrangian for a spin-two field in flat space, presented in [59], is given by

$$\mathcal{L} = \frac{1}{4}[-\partial_\rho B_{\mu\nu} \partial^\rho B^{\mu\nu} + 2B_\mu B^\mu - 2B^\mu \partial_\mu B^\alpha_\alpha + \partial_\mu B^\alpha_\alpha \partial^\mu B^\alpha_\alpha - m^2(B_{\mu\nu} B^{\mu\nu} - B^\alpha_\alpha B^\alpha_\alpha)], \quad (2.1)$$

where $B_\mu = \partial^\alpha B_{\alpha\mu}$. Since the tensor field $B_{\mu\nu}$ represents a spin-two field, it naturally follows that $B_{\mu\nu}$ is symmetric tensor field. For $d = 4$, the number of independent components of $B_{\mu\nu}$ are 10. The physical degree of freedom of a field with spin s is $2s + 1$ assuming that the field is massive. Therefore, we need five constraints equation for $B_{\mu\nu}$. The Fierz-Pauli Lagrangian is designed such that the necessary constraints are obtained as the consequence of the equations of motion (EOMs) and their derivatives. It is good idea to remind that for a massive spin one field A_μ , the constraint equation $\nabla_\mu A^\mu = 0$ is derived by taking a derivative of equation of motion of A_μ , which results in three physical degree of freedom of spin one field. In similar fashion, we can derive the constraint equations for a spin-two field. The EOM from the Fierz-Pauli Lagrangian is given as follows:

$$\partial^2 B_{\mu\nu} - \partial_\alpha \partial_\mu B^\alpha_\nu - \partial_\alpha \partial_\nu B^\alpha_\mu + \partial_\mu \partial_\nu B^\alpha_\alpha + \eta_{\mu\nu} \partial^\alpha \partial^\beta B_{\alpha\beta} - \eta_{\alpha\beta} \partial^2 B^\alpha_\alpha - m^2(B_{\mu\nu} - \eta_{\mu\nu} B^\alpha_\alpha) = 0, \quad (2.2)$$

where $\eta_{\mu\nu}$ is the flat space metric. By taking divergence on Eq. (2.2), we derive

$$\partial^\mu B_{\mu\nu} - \partial_\nu B^\alpha_\alpha = 0. \quad (2.3)$$

Substituting Eq. (2.3) in Eq. (2.2), we get

$$\partial^2 B_{\mu\nu} - \partial_\mu \partial_\nu B^\alpha_\alpha - m^2(B_{\mu\nu} - \eta_{\mu\nu} B^\alpha_\alpha) = 0. \quad (2.4)$$

Contracting with $\eta_{\mu\nu}$ in the above equation leads to the traceless condition of spin-two field $B^\alpha_\alpha = 0$. Substituting the traceless condition into Eq. (2.3), we get the transverse condition $\partial^\mu B_{\mu\nu} = 0$. We now have five constraints equations, which are traceless and transverse conditions, as a consequence of EOMs. This yields five independent components of the symmetric tensor field $B_{\mu\nu}$, which is the physical degree of freedom of spin-two field. The final equation of motion of spin-two field along with constraints in flat space reads

$$\partial^\alpha \partial_\alpha B_{\mu\nu} - m^2 B_{\mu\nu} = 0, \quad (2.5)$$

$$\partial_\mu B^{\mu\nu} = 0, \quad \text{and} \quad B^\mu_\mu = 0. \quad (2.6)$$

This yields the correct number of degrees of freedom for the dynamics of a spin-two field in flat space. The generalization of the above procedure in curved spacetime is nontrivial since the noncommutativity of the covariant derivatives introduces curvature dependent terms. The Lagrangian construction for a neutral massive spin-two field in curved spacetime with correct counting of the degrees of freedom was developed in [55] using two distinct methods. In one approach, the condition of vanishing Einstein tensor, $G_{\mu\nu} = 0$, was employed. In this scenario, all matter fields cannot exert a backreaction on the metric. In the alternate method, the static background condition was adopted to ensure the consistency of constraint equations, allowing matter fields to affect the metric. A detailed analysis of the Reissner-Nordstrom black hole solution was presented in [55]. We closely follow the procedure in [55] where the Lagrangian for a charged massive spin-two field in AdS spacetime was formulated under the Einstein condition, as described in [20]. We argue that the Einstein condition can be replaced by the traceless condition of the field, which is one of the constraints equation of the field. Then the backreaction of matter fields can be considered. The Lagrangian for a symmetric tensor in curved space can be expressed as follows [20]:

$$\begin{aligned} \mathcal{L} = & -|D_\rho B_{\mu\nu}|^2 + 2|D_\mu B^{\mu\nu}|^2 + |D_\mu B^\rho_\rho|^2 - (D_\mu B^{*\mu\nu} D_\nu B^\rho_\rho + \text{H.c.}) - m^2(|B_{\mu\nu}|^2 - |B^\mu_\mu|^2) \\ & + c_1 R_{\mu\nu\rho\lambda} B^{*\mu\rho} B^{\nu\lambda} + c_2 R_{\mu\nu} B^{*\mu\rho} B^\nu_\rho + c_3 R |B_{\mu\nu}|^2 + iqc_4 F_{\mu\nu} B^{*\mu\rho} B^\nu_\rho + c_5 R |B^\rho_\rho|^2 \\ & + c_6 (e^{i\phi} R_{\mu\nu} B^{*\mu\nu} B^\rho_\rho + \text{H.c.}), \end{aligned} \quad (2.7)$$

where $B_\mu = D^\alpha B_{\alpha\mu}$ and $R_{\mu\nu\rho\lambda}$, $R_{\mu\nu}$, R are the Riemann tensor, Ricci curvature, and Ricci scalar of the background spacetime, respectively. The corresponding equation of motion

$$\begin{aligned}
E_{\mu\nu} = & (D^\alpha D_\alpha - m^2)B_{\mu\nu} - (D_\mu B_\nu + D_\nu B_\mu) + \frac{1}{2}(D_\mu D_\nu B^\rho{}_\rho + D_\nu D_\mu B^\rho{}_\rho) + g_{\mu\nu}D^\alpha B_\alpha \\
& - g_{\mu\nu}(D^\alpha D_\alpha - m^2)B^\rho{}_\rho + c_1 R_{\mu\rho\nu\lambda}B^{\rho\lambda} + \frac{c_2}{2}(R_{\mu\alpha}B^\alpha_\nu + R_{\nu\alpha}B^\alpha_\mu) + c_3 R B_{\mu\nu} \\
& + c_4 \frac{iq}{2}(F_{\mu\alpha}B^\alpha_\nu + F_{\nu\alpha}B^\alpha_\mu) + c_5 g_{\mu\nu}R B^\rho{}_\rho + c_6(e^{i\phi}R_{\mu\nu}B^\rho{}_\rho + e^{-i\phi}g_{\mu\nu}R_{\alpha\beta}B^{\alpha\beta}) = 0.
\end{aligned} \tag{2.8}$$

We now try to calculate all the coefficient c_i from the constraint equation $D^\mu D^\nu E_{\mu\nu} = 0$, which gives [20]

$$\begin{aligned}
(c_1 - 2)R^{\mu\alpha\nu\beta}D_\mu D_\nu B_{\alpha\beta} + c_2 R^{\mu\alpha}D_\mu B_\alpha + (c_3 R - m^2)D^\alpha B_\alpha + iq(1 + c_4)F^{\alpha\beta}D_\alpha B_\beta \\
+ (c_5 R + m^2)D^\mu D_\mu B^\rho{}_\rho + c_6 e^{-i\phi}R^{\alpha\beta}D^\mu D_\mu B_{\alpha\beta} + (1 + c_6 e^{i\phi})R^{\mu\alpha}D_\mu D_\alpha B^\rho{}_\rho + \dots = 0,
\end{aligned} \tag{2.9}$$

where the ellipsis denotes terms that contain at most a single derivative of the spin-two field. Since no second derivative term exists in any constraint equation, all terms involved in second-order derivatives in the above equation must vanish. This leads to contradictory equations for c_6 . To remove this contradiction, we use the traceless condition of the spin two field ($B^\rho{}_\rho = 0$) instead of the Einstein condition. Substituting $B^\rho{}_\rho = 0$ in the above equation, we get

$$\begin{aligned}
(c_1 - 2)R^{\mu\alpha\nu\beta}D_\mu D_\nu B_{\alpha\beta} + c_2 R^{\mu\alpha}D_\mu B_\alpha + (c_3 R - m^2)D^\alpha B_\alpha \\
+ iq(1 + c_4)F^{\alpha\beta}D_\alpha B_\beta + c_6 e^{-i\phi}R^{\alpha\beta}D^\mu D_\mu B_{\alpha\beta} + \dots = 0.
\end{aligned} \tag{2.10}$$

The above equation becomes a constraint equation when all second derivative terms are eliminated, which leads

$$\begin{aligned}
c_1 = 2, \quad c_2 = 0, \quad c_3 = 0, \quad c_4 = -1, \\
c_6 = 0, \quad \text{and} \quad m^2 = 0.
\end{aligned} \tag{2.11}$$

In the above method, we have not used Einstein condition to determine c_i . Therefore, we can consider the backreaction of the matter field on the background geometry. The Lagrangian for a traceless symmetric spin-two field with Maxwell's term then is given by

$$\begin{aligned}
\mathcal{L}_m = & -|D_\alpha B_{\mu\nu}|^2 + 2|D_\mu B^{\mu\nu}|^2 + 2R_{\mu\rho\nu\lambda}B^{*\mu\rho}B^{\nu\lambda} \\
& - iqF_{\mu\nu}B^{*\mu\lambda}B^\nu_\lambda - \frac{1}{4}F_{\mu\nu}F^{\mu\nu}.
\end{aligned} \tag{2.12}$$

III. HOLOGRAPHIC d -WAVE SUPERCONDUCTOR

The action for d -wave holographic superconductors reads

$$S = \frac{1}{2\kappa^2} \int d^4x \sqrt{-g} [R - 2\Lambda + 2\kappa^2 \mathcal{L}_m], \tag{3.1}$$

where Λ is the cosmological constant and κ^2 is the gravitational Newton constant. The equation of motions for the tensor field and gauge field yield

$$\begin{aligned}
\Box B_{\alpha\beta} - (D_\alpha B_\beta + D_\beta B_\alpha) + 2R_{\alpha\mu\beta\nu}B^{\mu\nu} \\
- \frac{iq}{2}(F_{\alpha\mu}B^\mu_\beta + F_{\beta\mu}B^\mu_\alpha) = 0,
\end{aligned} \tag{3.2}$$

$$D_\mu F^{\mu\nu} - [iqB_{\alpha\beta}^*(D^\nu B^{\alpha\beta} - D^\alpha B^{\nu\beta}) + iqB_\alpha^* B^{\nu\alpha} + \text{H.c.}] = 0 \tag{3.3}$$

The Einstein field reads

$$R_{\alpha\beta} - \frac{1}{2}g_{\alpha\beta}R + \Lambda g_{\alpha\beta} = 2\kappa^2 T_{\alpha\beta}, \tag{3.4}$$

where $T_{\alpha\beta} = \frac{1}{2}g_{\alpha\beta}\mathcal{L}_m - \frac{\delta\mathcal{L}_m}{\delta g^{\alpha\beta}}$. Considering the backreacted four-dimensional metric in the following simplified form:

$$ds^2 = \frac{L^2}{z^2} \left[-f(z)g(z)dt^2 + \frac{dz^2}{f(z)} + dx^2 + dy^2 \right], \tag{3.5}$$

where L is the AdS radius. For this given black hole geometry, the Hawking temperature is

$$T_H = \frac{|f'(z_h)|\sqrt{g(z_h)}}{4\pi}. \tag{3.6}$$

To introduce both symmetry $d_{x^2-y^2}$ and d_{xy} in the system, we consider the tensor field in following form:

$$B = \frac{L^2\phi(z)}{\sqrt{2}z^2} [\alpha(dx^2 - dy^2) + 2\beta dx dy]. \tag{3.7}$$

When $\alpha = 0$ ($\beta = 0$), we will get only d_{xy} ($d_{x^2-y^2}$) symmetry. The matter field ansatz in general reads

$$B = B_{xx}(z)dx^2 + B_{xy}(z)dx dy + B_{yx}(z)dy dx + B_{yy}(z)dy^2. \tag{3.8}$$

Using the symmetric and traceless condition of the spin-two field, the above matter field ansatz in polar coordinate becomes

$$B = B_{\rho\rho}d\rho^2 + 2B_{\rho\theta}d\rho d\theta + B_{\theta\theta}d\theta^2, \quad (3.9)$$

where

$$\begin{aligned} B_{\rho\rho} &= \cos 2\theta B_{xx} + \sin 2\theta B_{xy}, \\ \frac{B_{\theta\theta}}{\rho^2} &= -\cos 2\theta B_{xx} + \sin 2\theta B_{xy}, \\ \frac{B_{\rho\theta}}{\rho} &= -\sin 2\theta B_{xx} + \cos 2\theta B_{xy}. \end{aligned} \quad (3.10)$$

Since $B_{\theta\theta}$ and $B_{\rho\theta}$ have coordinate singularity, the angle dependent order parameter for d -wave superconductor is $B_{\rho\rho}$. With the tensor field ansatz (3.7), the corrected order parameter reads

$$B_{\rho\rho} = \frac{L^2\phi(z)}{\sqrt{2}z^2} [\alpha \cos 2\theta + \beta \sin 2\theta]. \quad (3.11)$$

With gauge field ansatz $A = A_t(z)dt$, equation of motion of all fields are

$$g'(z) + 2\kappa^2 z d_m^2 \left[g(z)\phi'(z)^2 + \frac{2g(z)\phi(z)^2}{z^2} + \frac{q^2 A_t(z)^2 \phi(z)^2}{f(z)^2} \right] = 0, \quad (3.12)$$

$$f'(z) - \frac{3f(z)}{z} + \frac{3}{z} + \frac{f(z)g'(z)}{2g(z)} + \frac{2\kappa^2}{z} d_m^2 \left[f(z)\phi(z)^2 - \frac{z^4 A_t'(z)^2}{4L^2 d_m^2 g(z)} \right] = 0, \quad (3.13)$$

$$A_t''(z) - \frac{g'(z)}{2g(z)} A_t'(z) - \frac{2q^2 L^2 d_m^2 \phi(z)^2}{z^2 f(z)} A_t(z) = 0, \quad (3.14)$$

$$\phi''(z) + \left[\frac{f'(z)}{f(z)} + \frac{g'(z)}{2g(z)} - \frac{2}{z} \right] \phi'(z) + \left[\frac{q^2 A_t(z)^2}{f(z)^2 g(z)} \right] \phi(z) = 0, \quad (3.15)$$

where $d_m^2 = |\alpha|^2 + |\beta|^2$. The horizon condition $f(z_h) = 0$ and Eq. (3.13) lead us to determine the Hawking temperature, which reads

$$T_H = \frac{3\sqrt{g(z_h)}}{4\pi z_h} \left[1 - \frac{\kappa^2}{3} \left(\frac{z_h^3 A_t'(z_h)^2}{2L^2 g(z_h)} \right) \right]. \quad (3.16)$$

At the boundary of this spacetime should be an asymptotically AdS spacetime that imposes the boundary condition on $g(z=0) = 1$. Therefore the field equations at the boundary becomes

$$A''(z) = 0 \quad \text{and} \quad \phi''(z) - \frac{2}{z}\phi'(z) = 0, \quad (3.17)$$

which gives the asymptotic behavior of the gauge field and vector field in terms of quantities of boundary theory in following way:

$$A_t(z) = \mu - \tilde{\rho}z \quad \text{and} \quad \phi(z) = C_s + C_c z^3, \quad (3.18)$$

where $\mu, \tilde{\rho}, C_s, C_c$ are the chemical potential, charge density, source term, and expectation value of angle independent condensation of the boundary theory, respectively. From Eq. (3.11), the angle dependent order parameter for the d -wave holographic superconductor can be mapped with the condensation value of the boundary theory in following way:

$$B_{\rho\rho} = \frac{L^2\phi(z)}{\sqrt{2}z^2} [\alpha \cos 2\theta + \beta \sin 2\theta] = \langle \mathcal{O} \rangle z \quad (3.19)$$

when the source (C_s) is zero. Therefore, the angle dependent condensation operator reads

$$\langle \mathcal{O} \rangle = \frac{L^2 C_c}{\sqrt{2}} [\alpha \cos 2\theta + \beta \sin 2\theta] = \frac{L^2 C_c l}{\sqrt{2}} \cos(2\theta - \theta_1), \quad (3.20)$$

where $l^2 = \alpha^2 + \beta^2$ and $\tan \theta_1 = \frac{\beta}{\alpha}$ are determined from the given value of real value α and β . The above expression clearly shows that the mixing of $d_{x^2-y^2}$ and d_{xy} symmetry in system rotates the gap structure. In order to determine the angle dependent condensation operator value, we now need to calculate the C_c value in the full backreacted system. This gives us momentum dependent gap structure in Fourier space (k_x, k_y) with help of the following identification:

$$\Delta_k = FT[\langle \mathcal{O} \rangle] = \frac{1}{2\pi a^2} \int_0^a \int_0^{2\pi} \langle \mathcal{O} \rangle e^{-i(k_x \rho \cos \theta + k_y \rho \sin \theta)} \rho d\rho d\theta, \quad (3.21)$$

where a is the sample size and $FT[\dots]$ is the two-dimensional Fourier transformation.

A. The critical temperature and momentum dependent order parameter

In this subsection, we will employ the Shooting method to numerically solve the system of coupled equations, given by Eqs. (3.12)–(3.15). With help of scaling symmetry [53,57] of the equation of motion of all fields, we can set $L = 1$ and $2\kappa^2 = 1$. To successfully solve these equations, it is essential to provide appropriate boundary conditions for all fields, which are

$$A_t(z_h) = 0, \quad f(z_h) = 0, \quad g(0) = 1, \quad C_s = 0. \quad (3.22)$$

By specifying (T, μ) parameters, we are able to obtain solutions for all the equations in the system. To unveil the near-horizon behavior of the fields, we employ a Taylor series expansion, allowing us to express the fields as follows:

$$(V_y(z), A_t(z), f(z), g(z)) \approx \sum_{i=0}^5 (V_{yi}, A_{ti}, f_i, g_i) \left(1 - \frac{z}{z_h}\right)^i. \quad (3.23)$$

By substituting the aforementioned expansion into the field equations, as given by Eqs. (3.12)–(3.15), we establish a relation between the coefficients $(V_{yi}, A_{ti}, f_i, g_i)$ and the horizon data $(V_{y0}, A_{t1}, z_h, g_0)$. Through the imposition of the boundary conditions and the subsequent solution of the equations of motion for the fields, we can determine the horizon data for a given combination of (T, μ) , denoted as (T_0, μ_0) . The utilization of these field equations, as presented in Eq. (3.23), in conjunction with the solution for the horizon data, yields the complete configurations of all fields for a desired ratio $\frac{T}{\mu}$.

With the choice of the charge of the tensor field $q = 2$, and utilizing Eq. (3.16), we have determined that $T_c \approx 0.02\mu$. Remarkably, this critical temperature remains consistent regardless of the symmetry parameter, whether it is for d_{xy} -wave ($\alpha = 0, \beta = 1$) superconductivity, or for $d_{x^2-y^2}$ -wave ($\alpha = 1, \beta = 0$) superconductivity, or for $(d_{x^2-y^2} + d_{xy})$ -wave ($\alpha = \frac{1}{\sqrt{2}}, \beta = \frac{1}{\sqrt{2}}$) superconductivity. Furthermore, for a fixed temperature, the condensation value is approximately $C_c \approx 0.05522\mu^3$ for all three types of superconductivity: d_{xy} wave, $d_{x^2-y^2}$ wave, and $d_{x^2-y^2} + d_{xy}$ wave. The field configurations are illustrated in Fig. 1. Moving forward, we employ this field solution and Eq. (3.21) to plot the momentum-dependent gap structure at $T = 0.125T_c$, as depicted in Fig. 2. Subsequently, in a subsequent section, we will explore the fermionic spectral function, which will exhibit a Fermi arc at a 45° angle in

momentum space for the $d_{x^2-y^2}$ -wave symmetry. This analysis will provide support for the proposition that the order parameter in d -wave holographic superconductors should be $B_{\rho\rho}$ instead of B_{xy} or B_{xx} .

IV. FERMION WITH TENSOR CONDENSATION

A. Fermionic setup

The fermionic action can be expressed as [20]

$$S_\psi = \int d^4x \sqrt{-g} [i\bar{\psi}(\Gamma^\mu D_\mu - m_f)\psi - i\bar{\psi}_c(\Gamma^\mu D_\mu^* - m_f)\psi_c + \mathcal{L}_{\text{int}}],$$

$$\mathcal{L}_{\text{int}} = \eta^* B_{\mu\nu}^* \bar{\psi}_c \Gamma^\mu D^\nu \psi - \eta \bar{\psi} \Gamma^\mu D^\nu (B_{\mu\nu} \psi_c). \quad (4.1)$$

Here, η represents the coupling constant. The spinor's covariant derivative is denoted by $D_\mu = \partial_\mu + \frac{1}{4} \omega_{\mu\alpha\beta} \Gamma^{\alpha\beta} - iq_f A_\mu$. Additionally, the field $\psi_c = \psi^*$ corresponds to the complex charge conjugate field of the fermion, which is treated as an independent field throughout the computations in this framework. The boundary action for standard quantization [60,61] is given by

$$S_{\text{bdy}} = i \int d^3x \sqrt{-h} (\bar{\psi} \psi + \bar{\psi}_c \psi_c). \quad (4.2)$$

For this formulation, we adopt the following set of bulk gamma matrices:

$$\Gamma^t = \sigma_1 \otimes i\sigma_2, \quad \Gamma^x = \sigma_1 \otimes \sigma_1, \quad \Gamma^y = \sigma_1 \otimes \sigma_3,$$

$$\Gamma^z = \sigma_3 \otimes \sigma_0, \quad (4.3)$$

where underline indices represent tangent space indices. We obtain the Dirac equation [20]

$$(\Gamma^\mu D_\mu - m_f)\psi + i\mathcal{I}_{\text{int}}\psi_c = 0, \quad (4.4)$$

where $\mathcal{I}_{\text{int}} = 2\eta B_{\mu\nu} \Gamma^\mu D^\nu + \eta B_\mu \Gamma^\mu$. To simplify the analysis, we express the fermionic field as follows:

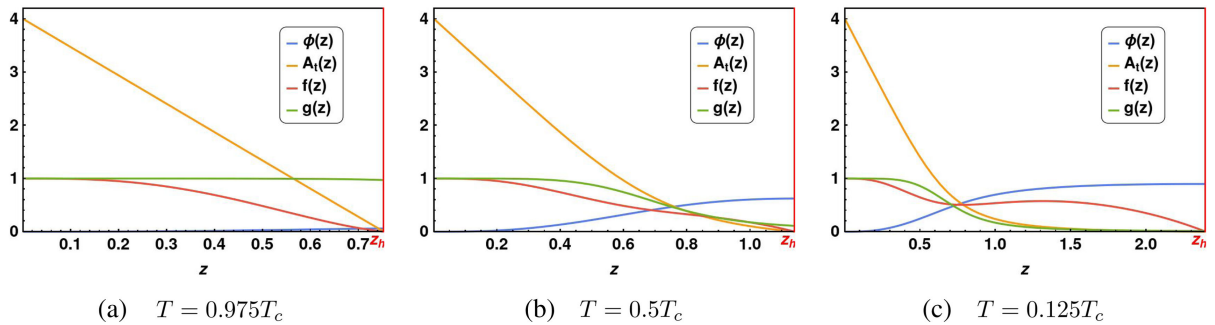
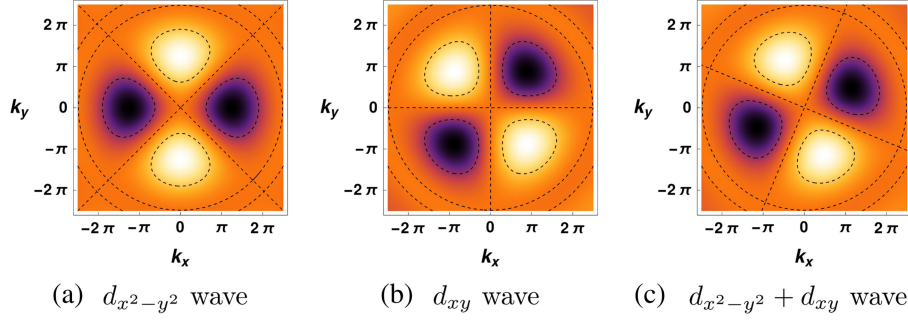


FIG. 1. Backreacted profiles at three different temperatures.

FIG. 2. Momentum dependent order parameter at $T = 0.125T_c$ for different symmetries.

$$\psi(t, x, y, z) = \frac{1}{(-gg^{zz})^{1/4}} e^{-i\omega t + ik_x x + ik_y y} \Psi(z). \quad (4.5)$$

This form allows us to eliminate the spin connection term in the spinor's equation of motion. By substituting the aforementioned spinor into the Dirac equations, we derive the following expressions:

$$\left[\Gamma^z \partial_z - i \left(\sqrt{\frac{g^{tt}}{g^{zz}}} (\omega + q_f A_t) \Gamma^t - \sqrt{\frac{g^{xx}}{g^{zz}}} k_x \Gamma^x - \sqrt{\frac{g^{yy}}{g^{zz}}} k_y \Gamma^y \right) - \frac{m_f}{\sqrt{g^{zz}}} \right] \Psi(z) + \frac{i}{\sqrt{g^{zz}}} \tilde{\mathcal{I}}_{\text{int}} \Psi_c(z) = 0, \quad (4.6)$$

where $\tilde{\mathcal{I}}_{\text{int}} = -\frac{\sqrt{2} \eta \phi(z)}{z^2} (g^{xx})^{\frac{3}{2}} [\alpha (k_x \Gamma^x - k_y \Gamma^y) + \beta (k_x \Gamma^y + k_y \Gamma^x)]$ since the metric is isotropic xy plane. The field equation for conjugate fermion is

$$\left[\Gamma^z \partial_z + i \left(\sqrt{\frac{g^{tt}}{g^{zz}}} (\omega - q_f A_t) \Gamma^t - \sqrt{\frac{g^{xx}}{g^{zz}}} k_x \Gamma^x - \sqrt{\frac{g^{yy}}{g^{zz}}} k_y \Gamma^y \right) - \frac{m_f}{\sqrt{g^{zz}}} \right] \Psi_c(z) - \frac{i}{\sqrt{g^{zz}}} \tilde{\mathcal{I}}_{\text{int}} \Psi(z) = 0. \quad (4.7)$$

We express the four-component spinor as

$$\Psi(z) = \begin{pmatrix} \Psi_+(z) \\ \Psi_-(z) \end{pmatrix}, \quad \text{where } \Psi_{\pm} = \begin{pmatrix} \Psi_{\pm 1} \\ \Psi_{\pm 2} \end{pmatrix}, \quad (4.8)$$

which allows us to formulate the Dirac equation as follows:

$$\left[\partial_z \mp \frac{m_f}{\sqrt{g^{zz}}} \right] \Psi_{\pm}(z) = \pm \left[i K_{\mu} \gamma^{\mu} \Psi_{\mp}(z) + \frac{\sqrt{2} \eta g^{xx} \phi(z)}{z^2} (\alpha K_{\mu} \gamma^{\mu}_{(\alpha)} + \beta K_{\mu} \gamma^{\mu}_{(\beta)}) \Psi_{c\mp}(z) \right], \quad (4.9)$$

where $K_{\mu} = \left(\sqrt{\frac{g^{tt}}{g^{zz}}} (\omega + q_f A_t), -\sqrt{\frac{g^{xx}}{g^{zz}}} k_x, -\sqrt{\frac{g^{yy}}{g^{zz}}} k_y \right)$, $\gamma^{\mu} = (i\sigma_2, \sigma_1, \sigma_3)$, $\gamma^{\mu}_{(\alpha)} = (0, \sigma_1, -\sigma_3)$, and $\gamma^{\mu}_{(\beta)} = (0, \sigma_3, \sigma_1)$. In a similar manner, we can reformulate the equation of motion for the conjugate fermion. In the asymptotic limit as $z \rightarrow 0$, we consider $g^{\mu\nu} \rightarrow z^2 \eta^{\mu\nu}$, where $\eta^{\mu\nu}$ is the Minkowski metric. Consequently, the behavior of the spinor in this regime is given by

$$\Psi_+(z) = \mathbf{A} z^{m_f} + \mathbf{B} z^{1-m_f}, \quad \Psi_-(z) = \mathbf{D} z^{-m_f} + \mathbf{C} z^{1+m_f}, \quad (4.10)$$

$$\Psi_{c+}(z) = \tilde{\mathbf{A}}^* z^{m_f} + \tilde{\mathbf{B}}^* z^{1-m_f}, \quad \Psi_{c-}(z) = \tilde{\mathbf{D}}^* z^{-m_f} + \tilde{\mathbf{C}}^* z^{1+m_f}. \quad (4.11)$$

Here, \mathbf{A} , \mathbf{B} , \mathbf{C} , \mathbf{D} are two-component spinors that are determined by solving the complete bulk Dirac equations. For $|m_f| < \frac{1}{2}$, the leading term yields the boundary spinor solutions as follows:

$$\Psi(z) \approx \begin{pmatrix} \mathbf{A} z^{m_f} \\ \mathbf{D} z^{-m_f} \end{pmatrix}, \quad \Psi_c(z) \approx \begin{pmatrix} \tilde{\mathbf{A}}^* z^{m_f} \\ \tilde{\mathbf{D}}^* z^{-m_f} \end{pmatrix}. \quad (4.12)$$

Remarkably, we have found that the leading order of the asymptotic behavior of the fields is always $z^{\pm m_f}$ for $|m_f| < \frac{1}{2}$, and this behavior remains independent of the interaction. The two-component spinor captures the influence of the interactions. Following same procedure as in [51], we can write down the boundary action in following form:

$$S_{bdy} = \int d^3x [\xi^{(C)\dagger} \tilde{\Gamma} \xi^{(S)} + \xi^{(S)\dagger} \tilde{\Gamma} \xi^{(C)}], \quad (4.13)$$

where the boundary gamma matrix $\tilde{\Gamma} = \sigma_0 \otimes (-\sigma_2)$ and the source and condensation are given by

$$\begin{aligned} \xi^{(S)} &= \begin{pmatrix} \Psi_+ \\ \Psi_{c-} \end{pmatrix} \stackrel{z \rightarrow 0}{=} \begin{pmatrix} \mathbf{A} z^{m_f} \\ \tilde{\mathbf{D}}^* z^{-m_f} \end{pmatrix} \\ \text{and } \xi^{(C)} &= \begin{pmatrix} \Psi_- \\ \Psi_{c+} \end{pmatrix} \stackrel{z \rightarrow 0}{=} \begin{pmatrix} \mathbf{D} z^{-m_f} \\ \tilde{\mathbf{A}}^* z^{m_f} \end{pmatrix}. \end{aligned} \quad (4.14)$$

This is the Namubu-Gorkov spinor representation, which represents the particle-hole symmetry.

B. Green function from flow equation

Rearranging all components of Eqs. (4.6) and (4.7), we can recast the Dirac equations in the following structure:

$$\partial_z \xi^{(S)} + \mathbb{M}_1 \xi^{(S)} + \mathbb{M}_2 \xi^{(C)} = 0, \quad (4.15)$$

$$\partial_z \xi^{(C)} + \mathbb{M}_3 \xi^{(C)} + \mathbb{M}_4 \xi^{(S)} = 0, \quad (4.16)$$

where 4×4 matrix $\mathbb{M}_i, i = 1, 2, 3, 4$ are determined from (4.6), (4.7). We have calculated those \mathbb{M}_i , which are

$$\begin{aligned} \mathbb{M}_1 &= \begin{pmatrix} \mathbb{N}_1 & \mathbb{P}_1 \\ -\mathbb{P}_1 & -\mathbb{N}_1 \end{pmatrix}, & \mathbb{M}_2 &= \begin{pmatrix} \mathbb{N}_2(q) & 0 \\ 0 & \mathbb{N}_2(-q) \end{pmatrix}, \\ \mathbb{M}_3 &= -\mathbb{M}_1, & \mathbb{M}_4 &= -\mathbb{M}_2, \end{aligned} \quad (4.17)$$

where

$$\begin{aligned} \mathbb{N}_1 &= -\frac{m_f}{z\sqrt{f(z)}} \mathbf{1}_{2 \times 2}, \\ \mathbb{P}_1 &= \frac{\sqrt{2}\eta\phi(z)}{\sqrt{f(z)}} \left[\alpha \begin{pmatrix} -k_y & k_x \\ k_x & k_y \end{pmatrix} + \beta \begin{pmatrix} k_x & k_y \\ k_y & -k_x \end{pmatrix} \right] \\ \mathbb{N}_2(q) &= \frac{i}{\sqrt{f(z)}} \begin{pmatrix} k_y & k_x - \frac{(\omega + qA_t(z))}{\sqrt{f(z)g(z)}} \\ k_x + \frac{(\omega + qA_t(z))}{\sqrt{f(z)g(z)}} & -k_y \end{pmatrix}. \end{aligned} \quad (4.18)$$

Following the procedure in [50,51], we get flow equation of bulk Green's function in the following form:

$$\begin{aligned} \partial_z \mathbb{G}(z) + \tilde{\Gamma} \mathbb{M}_3 \tilde{\Gamma} \mathbb{G}(z) - \mathbb{G}(z) \mathbb{M}_1 - \mathbb{G}(z) \mathbb{M}_2 \tilde{\Gamma} \mathbb{G}(z) \\ + \tilde{\Gamma} \mathbb{M}_4 = 0. \end{aligned} \quad (4.19)$$

From the horizon behavior of spinor, we can find the horizon value of the bulk Green's function [50]

$$\mathbb{G}(z_h) = i \mathbf{1}_{4 \times 4}. \quad (4.20)$$

The boundary retarded Green's function is determined the solution of bulk Green's function at the boundary as follows:

$$\mathbb{G}_r = \lim_{z \rightarrow 0} U(z) \mathbb{G}(z) U(z), \quad (4.21)$$

where $U(z) = \text{diag}(z^m, z^m, z^{-m}, z^{-m})$ and \mathbb{G}_r is the retarded Green function, defined from the boundary action [60]. For the numerical evaluation of the Green function, we will fix the mass of the fermion to be zero ($m_f = 0$) and charge of fermion to be 1 since $q = 2q_f$. The fermionic spectral function is defined as

$$A(\omega, k_x, k_y) = \text{Tr}[\text{Im}[\mathbb{G}_r]]. \quad (4.22)$$

In the presence of fully backreacted bosonic fields, we will study the spectral function and will compare the spectral function in probe limit case with backreaction case in the next section.

V. FERMIONIC GAP IN THE PRESENCE OF TENSOR CONDENSATION

To incorporate the Fermi arc characteristic into holographic superconductors, we need to examine the fermionic spectral function within the framework of holographic superconductors. To acquire the fermionic spectral function, we employ numerical methods to solve the flow equation (4.19), utilizing the bulk Green function (4.20) evaluated at the horizon. In the probe limit, we examine the fermionic spectral function in the AdS-Schwarzschild background, wherein the influence of the bosonic matter field on the underlying spacetime is disregarded. In the absence of any bosonic condensate, the holographic fermion setup unveils a Fermi surface, whose Fermi momentum is dictated by the chemical potential. The emergence of the gap feature necessitates the introduction of interactions between the fermion field and a bosonic field.

By considering the tensor field interaction with fermions, we derive the d -wave fermionic spectral function, as depicted in Fig. 3, for the $d_{x^2-y^2}$ -orbital symmetry with the coupling constant $\eta = 1$ at $T = 0.125T_c$. In the plot of ω versus $k_x = k_y = k$ (at the 45° angle), no gap is observed, while a nonzero fermionic gap is evident in the ω versus k_x plot. This arises due to the order parameter being zero at 45° and maximal at 0° in momentum space. Consequently, the k_x -versus- k_y plot displays a Fermi arc along the 45° angle in momentum space for the $d_{x^2-y^2}$ symmetry. The spectral function's band represents the particle and hole bands, where the fermionic gap is defined as the gap in ω within these two bands. For d_{xy} symmetry, the position of the Fermi arc is shifted by approximately 45° from that of $d_{x^2-y^2}$. Moreover, a mixture of both symmetries leads to an additional rotation of the Fermi arc by approximately 22.5°

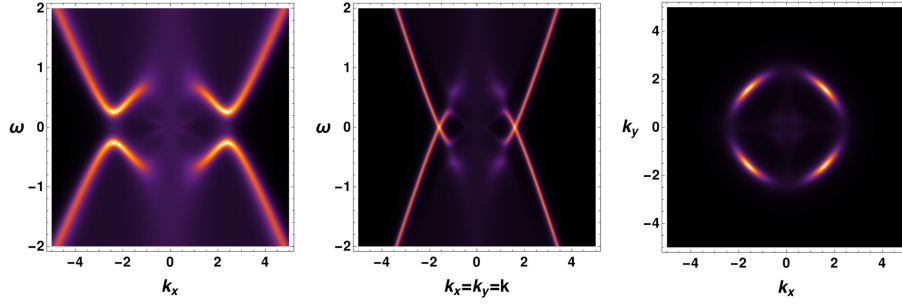


FIG. 3. Spectral function for $d_{x^2-y^2}$ condensate ($\alpha = 1, \beta = 0, \eta = 1$) at $T = 0.125T_c$.

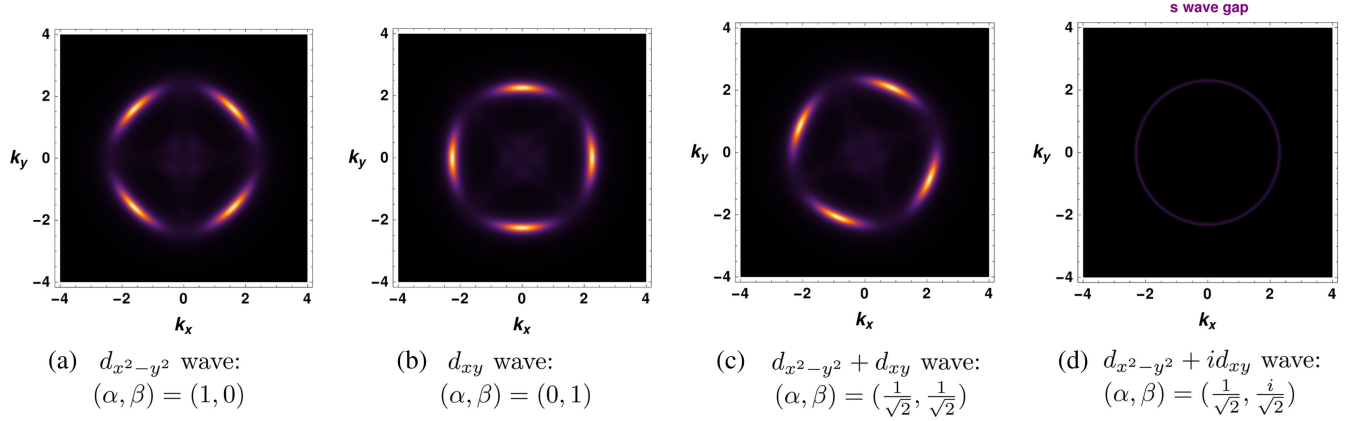


FIG. 4. Fermi arc in spectral function at $T = 0.125T_c$ with different d -wave symmetries. The $d_{x^2-y^2} + id_{xy}$ wave gives a s -wave fermionic spectral function.

compared to $d_{x^2-y^2}$, as demonstrated in Eq. (3.20) and Figs. 2, 4. Therefore, we can confirm that, in this holographic setup, the corrected angle-dependent order parameter is $B_{\rho\rho}$ rather than B_{xx} or B_{xy} .

Now we provide a comparative analysis of the fermionic spectral function between the probe limit scenario in our model and the case with backreaction, depicted in Fig. 5, considering $\eta = 1$ at $T = 0.125T_c$. Here, we have considered Schwarzschild-AdS black hole as a fixed background for the probe limit case. The probe limit in our Lagrangian leads to the same solution as in previous literature [20] for the same set of parameters. This

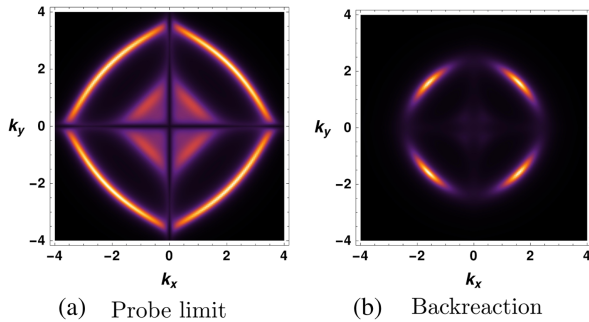
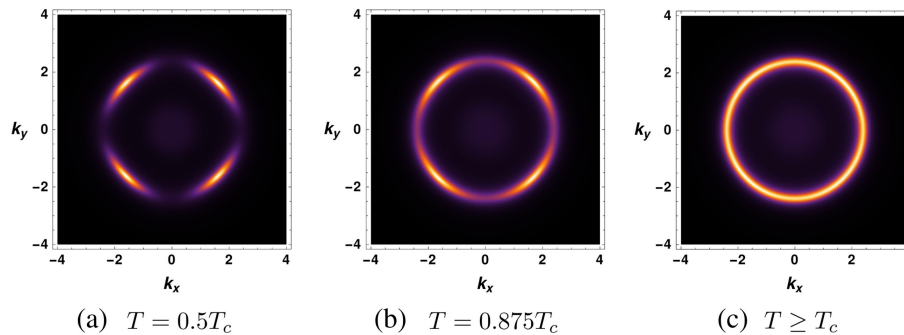
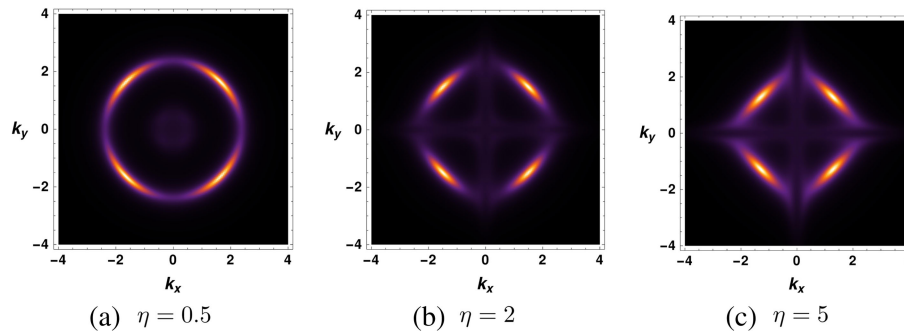


FIG. 5. Spectral function in probe limit case and backreacted cases at $T = 0.125T_c$.

illustration vividly demonstrates that the presence of backreaction exerts a substantial influence on the fermionic spectral function. Notably, the introduction of backreaction helps nullify the nonzero values of the spectral function inside the arc region.

We also aim to explore the impact of the temperature-to-chemical-potential ratio on the fermionic spectral function. We have investigated the ω gap manifested in the fermionic spectral function, which directly correlates with the magnitude of the order parameter. Through the examination of bosonic configuration, we know that the value of the order parameter decreases as the temperature rises, eventually reaching zero at the critical temperature T_c and beyond. Correspondingly, the fermionic gap decreases as the temperature increases, eventually vanishing at T_c , as illustrated in Fig. 6. Figure 7 shows the influence of the tensor interaction strength on the fermionic gap. It is apparent that the Fermi arc deforms a little bit for higher value of coupling strength. The gap amplifies in magnitude as the coupling strength increases. The ARPES data [1] shows that the structure of Fermi arc depends on the doping strength. Therefore, the coupling strength can be related with the doping parameter in the boundary theory.

To know the role of two flavor fermions in this setup, which is related to sublattice symmetry in real materials, we have explored two flavor fermions with two different

FIG. 6. Effect of temperature on spectral function with $d_{x^2-y^2}$ -condensate for $\eta = 1$.FIG. 7. Evolution of spectral function with the coupling strength at $T = 0.125T_c$.

condensate in the Appendix. We have found that two fermion flavors with condensates of two different tensor fields lead to higher orbital spectral function.

VI. DISCUSSION

In this paper, we have done a comprehensive examination of the fermionic spectral function under the influence of a fully backreacted tensor condensation. We have determined the critical temperature to be $T_c = 0.02\mu$ for the scaling dimension three and obtained all backreacted field configurations below this critical temperature. By employing these field configurations along with tensor interactions of different orbital symmetries, specifically $d_{x^2-y^2}$, d_{xy} , and a combination of $d_{x^2-y^2}$ and d_{xy} , we have conducted numerical investigations into the fermionic spectral function. This has been accomplished by solving the flow equation for the bulk Green function. Our analysis has unveiled the presence of a d -wave Fermi arc in the presence of the tensor field.

The momentum dependent order parameter, denoted as Δ_k , is identified as angle-dependent tensor field component $B_{\rho\rho}$ in momentum space. Comparing the momentum dependence of the order parameter (Fig. 2) with that of the fermion spectral function (Fig. 4), we confirm the correct order parameter for d -wave holographic superconductors. The $(d_{x^2-y^2} + d_{xy})$ -wave condensation rotates the Fermi arc position which confirms the d -wave order

parameter (3.20). We compare the spectral function in the probe limit case with the backreacted case. The $(d + id)$ -wave condensation leads the s -wave fermionic gap that exactly matches with previous findings [53]. Similarly, the $(p + ip)$ -wave condensation creates the s -wave fermionic spectral function.

The higher value of the coupling constant decreases the convexity of the Fermi arc. We have observed that as the temperature increases, the condensation value decreases, leading to a reduction in the fermionic gap. When the system reaches its critical temperature, it undergoes a transition to the normal phase. This transition is characterized by the emergence of a Fermi surface in the spectral function, attributed to the closure of the superconducting gap. The spectral function closely aligns with the experimental findings for high T_c superconductors mentioned in [1]. Furthermore, we have analyzed the role of two-flavor fermions in the presence of a vector field and a tensor field, resulting in a higher orbital symmetric fermionic spectral function. The vector condensate in the p_x and p_y directions, combined with two-flavor fermions, leads to a d -wave fermionic spectral function. Moreover, the combination of two d -wave symmetries ($d_{x^2-y^2}$ and d_{xy}) with two-flavor fermions results in a g -wave-like fermionic spectral function. This may have implications for the discovery of superconductivity with higher orbital symmetry. For the study of the unconventional superconductors within a holographic framework, the constructing the superconducting dome

through an examination of the spectral function is an intriguing avenue, which is our future direction.

ACKNOWLEDGMENTS

This work is supported by Mid-career Researcher Program through the National Research Foundation of Korea Grants No. NRF-2021R1A2B5B02002603, No. RS-2023-00218998, and No. NRF-2022H1D3A3A01077468. We thank the APCTP for the hospitality during the focus program, where part of this work was discussed.

APPENDIX: TWO FLAVOR FERMIONS: HIGHER ORBITAL SPECTRAL FUNCTION

Here, we delve into the investigation of two-flavor fermions within the context of vector and tensor condensation. The underlying motivation for exploring this scenario is to know whether the combination of two condensates with two-flavor fermions results in a spectral function exhibiting higher or lower orbital symmetry.

1. With tensor field

For tensor field, we have considered $d_{x^2-y^2}$ condensate with flavor one fermion and d_{xy} condensate with another flavor fermion. The corresponding interaction Lagrangian density is

$$\mathcal{L}_{\text{int}} = \sum_{i=1,2} [\eta^* B_{\mu\nu}^{*(i)} \bar{\psi}_c^{(i)} \Gamma^\mu D^\nu \psi^{(i)} - \eta \bar{\psi}^{(i)} \Gamma^\mu D^\nu (B_{\mu\nu}^{(i)} \psi_c^{(i)})], \quad (\text{A1})$$

where i is the flavor index, and $B^{(1)} = \frac{\alpha\phi(z)}{\sqrt{2z^2}} [dx^2 - dy^2]$ has $d_{x^2-y^2}$ symmetry and $B^{(2)} = 2\frac{\beta\phi(z)}{\sqrt{2z^2}} dx dy$ has d_{xy} symmetry. We can easily promote our previous calculation (one flavor) to two flavor by promoting the source and condensation in following form

$$\xi^{(C)} = \begin{pmatrix} \Psi_-^{(1)} \\ \Psi_-^{(2)} \\ \Psi_{c+}^{(1)} \\ \Psi_{c+}^{(2)} \end{pmatrix}, \quad \text{and} \quad \xi^{(S)} = \begin{pmatrix} \Psi_+^{(1)} \\ \Psi_+^{(2)} \\ \Psi_{c-}^{(1)} \\ \Psi_{c-}^{(2)} \end{pmatrix}. \quad (\text{A2})$$

The above expression is defined from following boundary action:

$$S_{bdy} = i \int d^3x \sqrt{-h} \sum_{i=1,2} [\bar{\psi}^{(i)} \psi^{(i)} + \bar{\psi}_c^{(i)} \psi_c^{(i)}]. \quad (\text{A3})$$

Using above setup, one can find a similar flow equation

$$\partial_z \mathbb{G}(z) + \tilde{\Gamma} \mathbb{M}_3 \tilde{\Gamma} \mathbb{G}(z) - \mathbb{G}(z) \mathbb{M}_1 - \mathbb{G}(z) \mathbb{M}_2 \tilde{\Gamma} \mathbb{G}(z) + \tilde{\Gamma} \mathbb{M}_4 = 0, \quad (\text{A4})$$

where $\mathbb{G}(z)$ is 8×8 bulk Green function matrix and all \mathbb{M}_i are given by

$$\mathbb{M}_1 = \begin{pmatrix} \mathbb{N}_1 & \mathbb{P}_1 \\ -\mathbb{P}_1 & -\mathbb{N}_1 \end{pmatrix}, \quad \mathbb{M}_2 = \begin{pmatrix} \mathbb{N}_2(q) & 0 \\ 0 & \mathbb{N}_2(-q) \end{pmatrix}, \quad \mathbb{M}_3 = -\mathbb{M}_1 \quad \mathbb{M}_4 = -\mathbb{M}_2, \quad (\text{A5})$$

where

$$\mathbb{N}_1 = -\frac{m_f}{z\sqrt{f(z)}} \mathbf{1}_{4 \times 4}, \quad \mathbb{P}_1 = \frac{\sqrt{2}\eta\phi(z)}{\sqrt{f(z)}} \begin{pmatrix} -\alpha k_y & \alpha k_x & 0 & 0 \\ \alpha k_x & \alpha k_y & 0 & 0 \\ 0 & 0 & \beta k_x & \beta k_y \\ 0 & 0 & \beta k_y & -\beta k_x \end{pmatrix}$$

$$\mathbb{N}_2(q) = \frac{i}{\sqrt{f(z)}} \begin{pmatrix} \mathbb{P}_2(q) & 0 \\ 0 & \mathbb{P}_2(q) \end{pmatrix} \quad \text{and} \quad \mathbb{P}_2(q) = \begin{pmatrix} k_y & k_x - \frac{(\omega + qA_t(z))}{\sqrt{f(z)g(z)}} \\ k_x + \frac{(\omega + qA_t(z))}{\sqrt{f(z)g(z)}} & -k_y \end{pmatrix}. \quad (\text{A6})$$

The horizon value of the bulk green function is $\mathbb{G}(z_h) = i\mathbf{1}_{8 \times 8}$. With this, we numerically calculated the spectral function in presence of backreaction that shows a g -wave like fermionic gap in the Fig. 8.

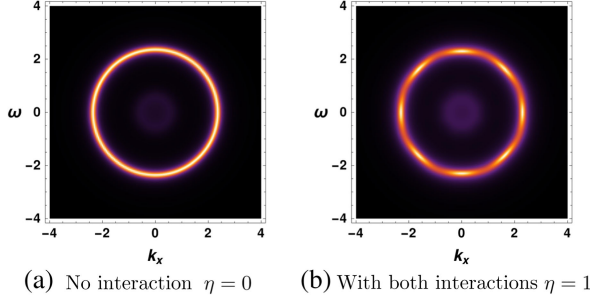


FIG. 8. The g -wave spectral function from two flavor fermions with two d -wave ($d_{x^2-y^2}$ and d_{xy}) condensate at $T = 0.125T_c$. (a) Fermi surface: when no interaction or one of interaction turn off ($\alpha = 0$ or $\beta = 0$). (b) The g wave: when both interactions turn on $\eta = 1$, $\alpha = \frac{1}{\sqrt{2}}$, $\beta = \frac{1}{\sqrt{2}}$, which means that flavor one is coupling with $d_{x^2-y^2}$ condensate and another flavor is coupling with d_{xy} condensate.

2. With vector field

Here, we start with one flavor fermion with p_x -wave and p_y -wave vector condensates. We will show that the $p_x + p_y$ wave rotates the Fermi arc position in momentum space. The Lagrangian for vector condensates reads

$$S_b = \int d^4x \sqrt{-g} \left[\frac{1}{2\kappa^2} (R - 2\Lambda) + \mathcal{L}_v \right], \quad (\text{A7})$$

where the matter Lagrangian density is

$$\mathcal{L}_v = -\frac{1}{4} F_{\mu\nu} F^{\mu\nu} - \frac{1}{2} V_{\mu\nu}^\dagger V^{\mu\nu} - m^2 V_\mu^\dagger V^\mu. \quad (\text{A8})$$

The covariant derivative of the vector field is defined as $V_{\mu\nu} = \partial_\mu V_\nu - \partial_\nu V_\mu - iq_\nu A_\mu V_\nu + iq_\nu A_\nu V_\mu$. With vector

field ansatz $V = \phi_p(z)[\tilde{\alpha}dx + \tilde{\beta}dy]$, we obtain

$$g' + \frac{2\kappa^2 z^3}{L^2} p_m^2 \left[g\phi_p'^2 + \frac{q_v^2 A_t^2 \phi_p^2}{f^2} \right] = 0, \quad (\text{A9})$$

$$f' - \frac{3}{z}f + \frac{3}{z} + \frac{g'}{2g}f - \kappa^2 z \left[m^2 p_m^2 \phi_p^2 + \frac{z^2 A_t'^2}{2L^2 g} \right] = 0, \quad (\text{A10})$$

$$A_t'' - \frac{g'}{2g}A_t' - \frac{2q_v^2 \phi_p^2}{f} p_m^2 A_t = 0, \quad (\text{A11})$$

$$\phi_p'' + \left[\frac{f'}{f} + \frac{g'}{2g} \right] \phi_p' + \left[\frac{q_v^2 A_t^2}{f^2 g} - \frac{m^2 L^2}{z^2 f} \right] \phi_p = 0, \quad (\text{A12})$$

where $p_m^2 = |\tilde{\alpha}|^2 + |\tilde{\beta}|^2$. Using horizon and boundary condition of the vector field [51], we solve all the four fields for a given value of $\frac{T}{\mu}$. The interaction between vector field and fermion is given by $\mathcal{L}_{\text{int}} = \bar{\psi} V_\mu \Gamma^\mu \psi_c + \text{H.c.}$ Using this interaction, we find the flow equation

$$\partial_z \mathbb{G}(z) + \tilde{\Gamma} \mathbb{M}_3 \tilde{\Gamma} \mathbb{G}(z) - \mathbb{G}(z) \mathbb{M}_1 - \mathbb{G}(z) \mathbb{M}_2 \tilde{\Gamma} \mathbb{G}(z) + \tilde{\Gamma} \mathbb{M}_4 = 0, \quad (\text{A13})$$

where the matrix \mathbb{M}_i is given by

$$\mathbb{M}_1 = \begin{pmatrix} \mathbb{N}_1 & \mathbb{P}_1 \\ \mathbb{P}_1 & -\mathbb{N}_1 \end{pmatrix}, \quad \mathbb{M}_2 = \begin{pmatrix} \mathbb{N}_2(q) & 0 \\ 0 & \mathbb{N}_2(-q) \end{pmatrix}, \\ \mathbb{M}_3 = -\mathbb{M}_1 \quad \mathbb{M}_4 = -\mathbb{M}_2, \quad (\text{A14})$$

where

$$\mathbb{N}_1 = -\frac{m_f}{z\sqrt{f(z)}} \mathbf{1}_{2 \times 2}, \quad \mathbb{P}_1 = \frac{i\phi_p(z)}{\sqrt{f(z)}} \left[\tilde{\alpha} \begin{pmatrix} 0 & -1 \\ -1 & 0 \end{pmatrix} + \tilde{\beta} \begin{pmatrix} -1 & 0 \\ 0 & 1 \end{pmatrix} \right] \\ \mathbb{N}_2(q) = \frac{i}{\sqrt{f(z)}} \begin{pmatrix} k_y & k_x - \frac{(\omega + qA_t(z))}{\sqrt{f(z)g(z)}} \\ k_x + \frac{(\omega + qA_t(z))}{\sqrt{f(z)g(z)}} & -k_y \end{pmatrix}. \quad (\text{A15})$$

The spectral function at $T = 0.233T_c$ is shown in Fig. 9 for $\Delta = 2(m^2 = 0)$ and $m_f = 0$. The $p_x + ip_y$ wave rotates the Fermi arc position which confirms again that the p -wave order parameter [51] is $V_\rho = \phi_p(z)[\tilde{\alpha} \cos \theta + \tilde{\beta} \sin \theta]$. An s -wave fermionic spectral function can be derived from the $(p_x + ip_y)$ -wave order parameter, similar to how we obtained it from the $(d_{x^2-y^2} + id_{xy})$ -wave order parameter.

a. Two flavor fermions with vector field

The interaction term of two flavor fermion with p_x and p_y vector condensate can be expressed in the following form:

$$\mathcal{L}_{\text{int}} = \sum_{i=1,2} [\bar{\psi}^{(i)} V_\mu^{(i)} \Gamma^\mu \psi_c^{(i)} + \text{H.c.}], \quad (\text{A16})$$

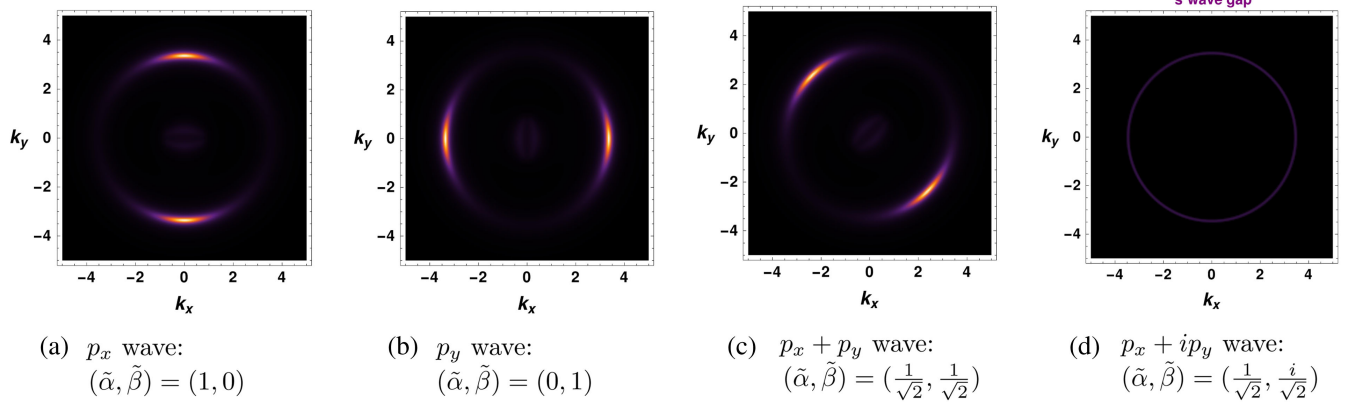


FIG. 9. One flavor fermionic spectral function with vector condensate at $T = 0.233T_c$. The plot (d) shows a s -wave fermionic spectral function from $(p_x + ip_y)$ -wave order parameter.

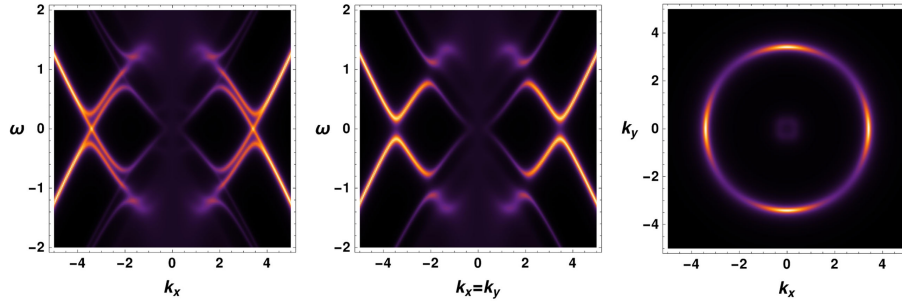


FIG. 10. Spectral function in the presence of the interaction of one flavor fermion with p_x -wave condensate and the interaction of another flavor fermion with p_y -wave condensate at $T = 0.233T_c$ shows a d -wave spectral function.

where $V^{(1)} = \tilde{\alpha}\phi_p(z)dx$ and $V^{(2)} = \tilde{\beta}\phi_p(z)dy$. The flow equation becomes

$$\partial_z \mathbb{G}(z) + \tilde{\Gamma} \mathbb{M}_3 \tilde{\Gamma} \mathbb{G}(z) - \mathbb{G}(z) \mathbb{M}_1 - \mathbb{G}(z) \mathbb{M}_2 \tilde{\Gamma} \mathbb{G}(z) + \tilde{\Gamma} \mathbb{M}_4 = 0, \quad (\text{A17})$$

where $\mathbb{G}(z)$ is 8×8 matrix and the matrix \mathbb{M}_i is given by

$$\mathbb{M}_1 = \begin{pmatrix} \mathbb{N}_1 & \mathbb{P}_1 \\ \mathbb{P}_1 & -\mathbb{N}_1 \end{pmatrix}, \quad \mathbb{M}_2 = \begin{pmatrix} \mathbb{N}_2(q) & 0 \\ 0 & \mathbb{N}_2(-q) \end{pmatrix}, \quad \mathbb{M}_3 = -\mathbb{M}_1 \quad \mathbb{M}_4 = -\mathbb{M}_2. \quad (\text{A18})$$

All 4×4 matrices in the above expression are given by

$$\mathbb{N}_1 = -\frac{m_f}{z\sqrt{f(z)}} \mathbf{1}_{4 \times 4}, \quad \mathbb{P}_1 = \frac{i\phi_p(z)}{\sqrt{f(z)}} \begin{pmatrix} 0 & -\tilde{\alpha} & 0 & 0 \\ -\tilde{\alpha} & 0 & 0 & 0 \\ 0 & 0 & -\tilde{\beta} & 0 \\ 0 & 0 & 0 & \tilde{\beta} \end{pmatrix},$$

$$\mathbb{N}_2(q) = \frac{i}{\sqrt{f(z)}} \begin{pmatrix} \mathbb{P}_2(q) & 0 \\ 0 & \mathbb{P}_2(q) \end{pmatrix}, \quad \mathbb{P}_2(q) = \begin{pmatrix} k_y & k_x - \frac{(\omega + qA_t(z))}{\sqrt{f(z)g(z)}} \\ k_x + \frac{(\omega + qA_t(z))}{\sqrt{f(z)g(z)}} & -k_y \end{pmatrix}. \quad (\text{A19})$$

The resulting spectral function is given in Fig. 10. This shows a clear d -wave fermionic spectral function from the interaction of flavor one with p_x -wave condensate and another flavor with p_y -wave condensate at $T = 0.233T_c$. Therefore, combining two condensates with two-flavor fermions gives a spectral function exhibiting higher orbital symmetry.

- [1] J. A. Sobota, Y. He, and Z.-X. Shen, Angle-resolved photoemission studies of quantum materials, *Rev. Mod. Phys.* **93**, 025006 (2021).
- [2] J. M. Maldacena, The large N limit of superconformal field theories and supergravity, *Int. J. Theor. Phys.* **38**, 1113 (1999).
- [3] S. S. Gubser, I. R. Klebanov, and A. M. Polyakov, Gauge theory correlators from noncritical string theory, *Phys. Lett. B* **428**, 105 (1998).
- [4] E. Witten, Anti-de Sitter space and holography, *Adv. Theor. Math. Phys.* **2**, 253 (1998).
- [5] S. A. Hartnoll, P. K. Kovtun, and M. S. Müller, Theory of the Nernst effect near quantum phase transitions in condensed matter and in dyonic black holes, *Phys. Rev. B* **76**, 144502 (2007).
- [6] Y. Seo, G. Song, P. Kim, S. Sachdev, and S.-J. Sin, Holography of the Dirac fluid in graphene with two currents, *Phys. Rev. Lett.* **118**, 036601 (2017).
- [7] E. Oh, T. Yuk, and S.-J. Sin, The emergence of strange metal and topological liquid near quantum critical point in a solvable model, *J. High Energy Phys.* **11** (2021) 207.
- [8] G. Song, J. Rong, and S.-J. Sin, Stability of topology in interacting Weyl semi-metal and topological dipole in holography, *J. High Energy Phys.* **10** (2019) 109.
- [9] E. Oh, Y. Seo, T. Yuk, and S.-J. Sin, Ginzberg-Landau-Wilson theory for Flat band, Fermi-arc and surface states of strongly correlated systems, *J. High Energy Phys.* **01** (2021) 053.
- [10] E. Oh and S.-J. Sin, Entanglement string and spin liquid with holographic duality, *Phys. Rev. D* **101**, 066020 (2020).
- [11] Y. Seo, G. Song, and S.-J. Sin, Strong correlation effects on surfaces of topological insulators via holography, *Phys. Rev. B* **96**, 041104 (2017).
- [12] Y. Seo, G. Song, Y.-H. Qi, and S.-J. Sin, Mott transition with holographic spectral function, *J. High Energy Phys.* **08** (2018) 077.
- [13] Y. Seo, G. Song, C. Park, and S.-J. Sin, Small Fermi surfaces and strong correlation effects in Dirac materials with holography, *J. High Energy Phys.* **10** (2017) 204.
- [14] K. K. Romes, A. Pasupathy, A. Pushp, S. Ono, Y. Ando, and A. Yazdani, Visualizing pair formation on the atomic scale in the high- T_c superconductor $\text{Bi}_2\text{Sr}_2\text{CaCu}_2\text{O}_{8+\delta}$, *Nature (London)* **447**, 569 (2007).
- [15] S. A. Hartnoll, C. P. Herzog, and G. T. Horowitz, Building a holographic superconductor, *Phys. Rev. Lett.* **101**, 031601 (2008).
- [16] S. S. Gubser, Breaking an Abelian gauge symmetry near a black hole horizon, *Phys. Rev. D* **78**, 065034 (2008).
- [17] S. S. Gubser and S. S. Pufu, The gravity dual of a p-wave superconductor, *J. High Energy Phys.* **11** (2008) 033.
- [18] D. Vegh, Fermi arcs from holography, [arXiv:1007.0246](https://arxiv.org/abs/1007.0246).
- [19] D. Ghorai, Y.-S. Choun, and S.-J. Sin, Momentum dependent gap in holographic superconductors revisited, *J. High Energy Phys.* **09** (2022) 098.
- [20] F. Benini, C. P. Herzog, R. Rahman, and A. Yarom, Gauge gravity duality for d-wave superconductors: Prospects and challenges, *J. High Energy Phys.* **11** (2010) 137.
- [21] J.-W. Chen, Y.-J. Kao, D. Maity, W.-Y. Wen, and C.-P. Yeh, Towards A holographic model of D-wave superconductors, *Phys. Rev. D* **81**, 106008 (2010).
- [22] H.-B. Zeng, Z.-Y. Fan, and H.-S. Zong, Characteristic length of a Holographic Superconductor with d -wave gap, *Phys. Rev. D* **82**, 126014 (2010).
- [23] D. Gao, Vortex and droplet in holographic D-wave superconductors, *Phys. Lett. A* **376**, 1705 (2012).
- [24] A. Krikun, Charge density wave instability in holographic d-wave superconductor, *J. High Energy Phys.* **04** (2014) 135.
- [25] M. Nishida, Phase diagram of a holographic superconductor model with s-wave and d-wave, *J. High Energy Phys.* **09** (2014) 154.
- [26] A. Krikun, Phases of holographic d-wave superconductor, *J. High Energy Phys.* **10** (2015) 123.
- [27] G. T. Horowitz and M. M. Roberts, Holographic superconductors with various condensates, *Phys. Rev. D* **78**, 126008 (2008).
- [28] G. T. Horowitz and M. M. Roberts, Zero temperature limit of holographic superconductors, *J. High Energy Phys.* **11** (2009) 015.
- [29] G. T. Horowitz, Introduction to holographic superconductors, in *From Gravity to Thermal Gauge Theories: The AdS/CFT Correspondence* (Springer, New York, 2011), pp. 313–347.
- [30] M. Ammon, J. Erdmenger, M. Kaminski, and A. O’Bannon, Fermionic operator mixing in holographic p-wave superfluids, *J. High Energy Phys.* **05** (2010) 053.
- [31] S. S. Gubser, F. D. Rocha, and A. Yarom, Fermion correlators in non-Abelian holographic superconductors, *J. High Energy Phys.* **11** (2010) 085.
- [32] S.-J. Sin, S.-S. Xu, and Y. Zhou, Holographic superconductor for a Lifshitz fixed point, *Int. J. Mod. Phys. A* **26**, 4617 (2011).
- [33] Y. Brihaye and B. Hartmann, Holographic superconductors in $3 + 1$ dimensions away from the probe limit, *Phys. Rev. D* **81**, 126008 (2010).
- [34] G. Siopsis and J. Therrien, Analytic calculation of properties of holographic superconductors, *J. High Energy Phys.* **05** (2010) 013.
- [35] H.-B. Zeng, Z.-Y. Fan, and H.-S. Zong, d-wave holographic superconductor vortex lattice and non-Abelian holographic superconductor droplet, *Phys. Rev. D* **82**, 126008 (2010).
- [36] G. Siopsis, Holographic superconductors at low temperatures, *Proc. Sci. CORFU2011* (2011) 078.
- [37] H.-B. Zeng, X. Gao, Y. Jiang, and H.-S. Zong, Analytical computation of critical exponents in several holographic superconductors, *J. High Energy Phys.* **05** (2011) 002.
- [38] Q. Pan, J. Jing, B. Wang, and S. Chen, Analytical study on holographic superconductors with backreactions, *J. High Energy Phys.* **06** (2012) 087.
- [39] G. Siopsis, J. Therrien, and S. Musiri, Holographic superconductors near the Breitenlohner–Freedman bound, *Classical Quantum Gravity* **29**, 085007 (2012).
- [40] S. Gangopadhyay and D. Roychowdhury, Analytic study of properties of holographic p-wave superconductors, *J. High Energy Phys.* **08** (2012) 014.
- [41] K.-Y. Kim and M. Taylor, Holographic d-wave superconductors, *J. High Energy Phys.* **08** (2013) 112.
- [42] R.-G. Cai, L. Li, and L.-F. Li, A holographic p-wave superconductor model, *J. High Energy Phys.* **01** (2014) 032.

- [43] O. DeWolfe, S. S. Gubser, O. Henriksson, and C. Rosen, Gapped fermions in top-down holographic superconductors, *Phys. Rev. D* **95**, 086005 (2017).
- [44] D. Ghorai and S. Gangopadhyay, Higher dimensional holographic superconductors in Born–Infeld electrodynamics with back-reaction, *Eur. Phys. J. C* **76**, 1 (2016).
- [45] D. Ghorai and S. Gangopadhyay, Holographic free energy and thermodynamic geometry, *Eur. Phys. J. C* **76**, 702 (2016).
- [46] A. Srivastav, D. Ghorai, and S. Gangopadhyay, p -wave holographic superconductors with massive vector condensate in Born-Infeld electrodynamics, *Eur. Phys. J. C* **80**, 219 (2020).
- [47] D. Ghorai and S. Gangopadhyay, Analytical study of holographic superconductor with backreaction in 4d Gauss-Bonnet gravity, *Phys. Lett. B* **822**, 136699 (2021).
- [48] A. Donini, V. Engueta-Vileta, F. Esser, and V. Sanz, Generalising holographic superconductors, *Adv. High Energy Phys.* **2022**, 1785050 (2022).
- [49] T. Faulkner, G. T. Horowitz, J. McGreevy, M. M. Roberts, and D. Vegh, Photoemission “experiments” on holographic superconductors, *J. High Energy Phys.* **03** (2010) 121.
- [50] T. Yuk and S.-J. Sin, Flow equation and fermion gap in the holographic superconductors, *J. High Energy Phys.* **02** (2023) 121.
- [51] D. Ghorai, T. Yuk, and S.-J. Sin, Fermi arc in p -wave holographic superconductors, *J. High Energy Phys.* **10** (2023) 003.
- [52] F. Benini, C.P. Herzog, and A. Yarom, Holographic Fermi arcs and a d-wave gap, *Phys. Lett. B* **701**, 626 (2011).
- [53] J.-W. Chen, Y.-S. Liu, and D. Maity, $d + id$ holographic superconductors, *J. High Energy Phys.* **05** (2011) 032.
- [54] I. L. Buchbinder, D. M. Gitman, V. A. Krykhtin, and V. D. Pershin, Equations of motion for massive spin-2 field coupled to gravity, *Nucl. Phys.* **B584**, 615 (2000).
- [55] I. L. Buchbinder, D. M. Gitman, and V. D. Pershin, Causality of massive spin-2 field in external gravity, *Phys. Lett. B* **492**, 161 (2000).
- [56] X.-H. Ge, S.F. Tu, and B. Wang, d-Wave holographic superconductors with backreaction in external magnetic fields, *J. High Energy Phys.* **09** (2012) 088.
- [57] Y. Xu, Y. Shi, D. Wang, and Q. Pan, Holographic entanglement entropy and complexity for D-wave superconductors, *Eur. Phys. J. C* **83**, 202 (2023).
- [58] S. A. Hartnoll, C. P. Herzog, and G. T. Horowitz, Holographic superconductors, *J. High Energy Phys.* **12** (2008) 015.
- [59] M. Fierz and W. Pauli, On relativistic wave equations for particles of arbitrary spin in an electromagnetic field, *Proc. R. Soc. A* **173**, 211 (1939).
- [60] N. Iqbal and H. Liu, Real-time response in AdS/CFT with application to spinors, *Fortschr. Phys.* **57**, 367 (2009).
- [61] J. N. Laia and D. Tong, A holographic flat band, *J. High Energy Phys.* **11** (2011) 125.